Astron. Astrophys. 318, 40–52 (1997)

ASTRONOMY
AND
ASTROPHYSICS

Luminosity and mass functions for the galactic globular cluster NGC 3201⋆

S. Covino[1] **and S. Ortolani**[2]

[1] Dip. di Fisica, Univ. di Milano, via Celoria 16, I-20133 Milano, Italy
[2] Dip. di Astronomia, Univ. di Padova, vicolo dell'Osservatorio 5, I-35122 Padova, Italy

Received 7 September 1995 / Accepted 10 June 1996

Abstract. Luminosity and mass functions for NGC 3201 down to $\sim 0.3\,M_{\odot}$ are derived from BV color–magnitude diagrams in different fields containing about $\sim 13\,000$ stars. We studied data for three independent fields observed with the NTT and 3.6m ESO telescopes and the derived mass functions are all in agreement with each other. Comparison with the data published in the literature have shown a fairly good agreement. This confirms that our results are quite reliable and that the completeness correction algorithm applied was substantially correct. From the observations taken at the Danish 1.5m ESO telescope we have determined a fiducial sequence from the giant and asymptotic branches down to the lower main–sequence (MS). This sequence is more extended than those previously reported. Reddening, metallicity, distance modulus and age have been obtained from composite c–m diagrams. A narrow sequence of blue straggler stars was also put into evidence.

Key words: globular clusters: NGC 3201 – stars: luminosity function, mass function – stars: population II – blue stragglers

1. Introduction

NGC 3201 [$\alpha_{2000} = 10^h17^m36.8^s$, $\delta_{2000} = -46^0 24' 40''$; $l_{II} = 277.228$, $b_{II} = 8.641$ Djorgovski & Meylan 1993] is a halo Globular Cluster (GC) rather close to the Sun ($d = 5$ kpc; Pryor & Meylan 1993) and with a relatively low concentration ($c = 1.31$; Trager et al. 1993). These combined features make it a prime target for investigation. The small distance modulus allows one to determine Luminosity and Mass Function (LF and MF) down to faint magnitudes, while the openess makes an investigation of its central region possible. In GC cores, in fact, it is possible to obtain a large sample of bright stars and to study rather peculiar objects as Blue Straggler Stars (BSS) and their progeny, i.e. stars that were formerly BSs (see Stryker 1993 for a review of the principal BSS formation mechanisms). Besides, the development of CCD technology and software capable of analyzing crowded fields has allowed observers to examine the faintest members of a GC. This kind of studies allow us to derive important information on the MF slope, the total mass–to–light ratio in GCs, and to investigate on the existence and on the location of a turnover in the LF. MF slopes can also provide further insights on the correlation recently singled out by Capaccioli et al. 1993 on MF slopes and the position of GCs in the Galactic gravitational field.

Previous photometric studies are those by Menzies 1967, Alcaino 1976, Lee 1977, Alcaino & Liller 1981, Cacciari 1984a and 1984b, Penny 1984, Alcaino et al. 1989, and Brewer et al. 1993. The last three are CCD–based photometric studies. See Table 1 for a summary of some estimated color–magnitude diagram parameters.

In Sect. 2 we describe the considered observational material and the reductions and calibrations performed, in Sect. 3 the analysed color–magnitude (c–m) diagrams and various related parameters as reddening, metallicity, distance modulus and age. In the last section (Sect. 4) we compute LFs and MFs from various fields in NGC 3201.

2. Observations, reductions and calibrations

Observations were taken at the European Southern Observatory (ESO) at La Silla with the NTT, 3.6m and 1.5 Danish telescopes. A brief journal of the observations is reported in Table 2.

One set of observations was carried out by the NTT telescope with EMMI (red and blue arms) equipped with a Ford CCD. Two fields in the cluster and one in the background were observed. The first (F1) was located at ~ 6 arcmin north–west from the cluster centre. The second (F2) was located at ~ 5 arcmin north–west from the cluster centre. They are both partially overlapped and have a size of $\sim 5 \times 5$ arcmin. The background field, of size of $\sim 8 \times 10$ arcmin, was located at ~ 34 arcmin west from the cluster centre.

Another set of observations was carried out at the focus of the EFOSC spectrograph at the 3.6m telescope in the focal reducer imaging mode.

Send offprint requests to: S. Ortolani

⋆ based on observations performed ESO–LA SILLA

Table 1. Some color–magnitude diagram parameters determined in previous photometric studies in NGC 3201.

V_{HB}	$E_{(B-V)}$	$\Delta V_{1.4}$	$(B-V)_{0,g}$	V_{TO}	$(B-V)_{TO}$	Ref.
14.9	0.07	2.6	0.77			Menzies 1967
14.7	0.14	2.6	0.81			Alcaino 1976
14.8	0.21	2.8	0.79			Lee 1977
14.67	0.22 ± 0.03	2.94	0.75	18.0	0.61	Alcaino & Liller 1981
14.76	0.21 ± 0.01					Cacciari 1984a, 1984b
14.6		2.9	0.83	18.1	0.70	Penny 1984
	0.20 ± 0.02			18.20 ± 0.1	0.57 ± 0.01	Alcaino et al. 1989
14.8 ± 0.15			0.77	18.25 ± 0.15	0.61 ± 0.03	Brewer et al. 1993

Table 2. Log of observations

date	Filter	Exposures time (min)	telescope	Field
1984 December 22	V	5	Danish	F5
1984 December 22	B	5	Danish	F5
1984 December 22	V	2	Danish	F7
1984 December 22	B	2	Danish	F7
1984 December 22	V	1	Danish	F7
1984 December 22	V	5	Danish	F6
1984 December 22	B	5	Danish	F6
1984 December 22	B	5	Danish	F6
1984 December 22	V	2	Danish	F6
1984 December 22	V	1	Danish	F7
1984 December 22	V	1	Danish	F7
1984 December 22	B	2	Danish	F7
1984 December 22	B	2	Danish	F7
1986 February 4–5	V	1	3.6	F3
1986 February 4–5	V	10	3.6	F3
1986 February 4–5	B	10	3.6	F3
1986 February 4–5	B	20	3.6	F3
1986 February 4–5	B	20	3.6	F3
1986 February 4–5	V	10	3.6	F3
1986 February 4–5	B	20	3.6	F3
1986 February 4–5	V	10	3.6	F3
1986 February 4–5	B	2	3.6	F3
1986 February 4–5	V	1	3.6	F3
1986 February 5–6	V	1	3.6	F4
1986 February 5–6	V	10	3.6	F4
1986 February 5–6	B	14	3.6	F4
1986 February 5–6	B	20	3.6	F4
1986 February 5–6	V	10	3.6	F4
1986 February 5–6	B	20	3.6	F4
1986 February 5–6	B	20	3.6	F4
1986 February 5–6	V	10	3.6	F4
1986 February 5–6	V	1	3.6	F4
1986 February 5–6	B	2	3.6	F4
1986 February 5–6	B	2	3.6	F4
1991 April 17	V	1	NTT	F1
1991 April 17	V	6	NTT	F2
1991 April 17	V	6	NTT	F2
1991 April 17	V	6	NTT	F2
1991 April 17	V	6	NTT	F2
1991 April 17	V	6	NTT	F2
1991 April 17	V	6	NTT	F2
1991 April 17	B	15	NTT	F2
1991 April 17	B	15	NTT	F2
1991 April 17	B	15	NTT	F2
1991 April 17	B	15	NTT	F2
1991 April 17	B	15	NTT	F2
1991 April 17	B	15	NTT	F2
1991 April 18	V	1	NTT	background
1991 April 18	V	1	NTT	background
1991 April 18	V	25	NTT	background
1991 April 18	V	25	NTT	background
1991 April 18	B	40	NTT	background
1991 April 18	B	40	NTT	background
1991 April 18	B	0.5	NTT	F1
1991 April 18	B	0.5	NTT	F1
1991 April 18	B	15	NTT	F2
1991 April 18	B	15	NTT	F2
1991 April 18	B	15	NTT	F2

The field F3 was located at some ~ 7 arcmin west from the cluster centre with size $\sim 3 \times 4$ arcmin. The field F4 was located at ~ 8 arcmin west from the cluster centre with the same size and with a small overlapping between the the previous field.

Three fields of $\sim 5 \times 4$ arcmin have been observed at the Danish 1.5m telescope. Namely, F5 at ~ 4.5 arcmin west from the cluster centre, F6 at ~ 2 arcmin west from the cluster centre and F7 on the cluster centre. All fields partially overlap one another.

Each observing run had average seeing conditions ($1 \div 1.5$ arcsec).

The frames reported in Table 2 have been averaged and the reductions have been carried out with the DAOPHOT II code (Stetson 1987) as available in the ESO–MIDAS package. We applied two full cycles of analysis (FIND–PHOTOMETRY–ALLSTAR) with an increasing detection threshold from the first to the second iteration. Point spread functions have been constructed for each frame using a large number of uncrowded stars, always greater than 10. Standard stars from Landolt 1983 were used for calibrations of NTT data. These stars were defocussed in order to avoid saturation and shutter timing problems. The frames taken at the 3.6m telescope have been calibrated computing the color term by observations of standard stars from Landolt 1983 while the zero–point has been derived using bright stars previously measured by Alcaino & Liller 1981. The observations taken at the Danish telescope have been calibrated using stars in common with the F1 NTT field. The relations between instrumental and calibrated magnitudes at the NTT telescope are:

$$\begin{aligned} V &= v + 0.04(B-V) + 2.89 \\ (B-V) &= 0.93(b-v) - 1.3, \end{aligned} \quad (1)$$

while those for the 3.6m telescope are:

$$\begin{aligned} V &= v + 3.75 \\ (B-V) &= 1.20(b-v) - 0.77. \end{aligned} \quad (2)$$

The errors are ~ 0.03 mag for NTT and ~ 0.05 for the 3.6m telescope.

Data are available on request by the authors.

3. Color–magnitude diagram

The c–m diagrams in Figs. 1 and 3 show a well defined MS at least down to $V \sim 22.5$. The fields analysed, whose c–m diagram is plotted in Fig. 1, do not cover the same area of the cluster. Consequently, the star counts along the post–MS stages and along the MS cannot be compared. Stars close to the turnoff (TO) in Fig. 3 and stars brighter than the horizontal branch (HB) in Fig. 1 are slightly saturated. A sharp BSS sequence almost up to the HB is also visible in Fig. 1.

The fiducial sequence for the MS, the red giant branch (RGB), the HB and the BSSs are reported in Table 3.

To get an estimate of the errors associated with the reported c–m diagrams we added ~ 1500 artificial stars to the F2 field

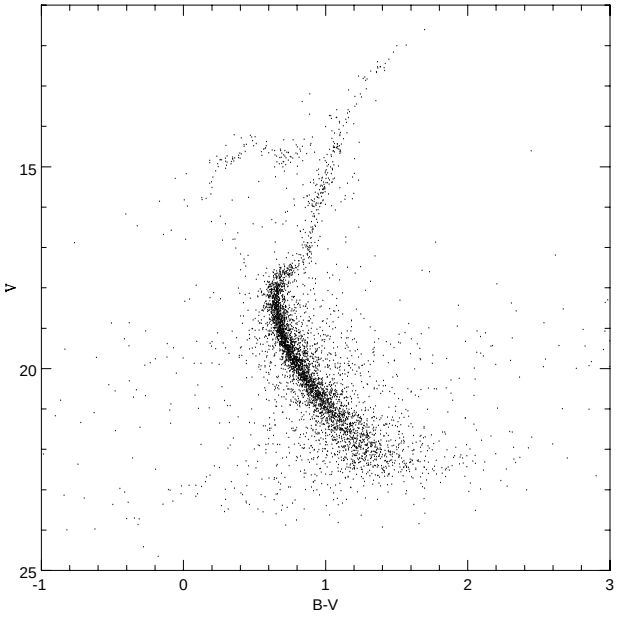

Fig. 1. Color–Magnitude diagram based on NTT observations for 5862 stars in the F2 frame and 2829 stars in the F5, F6 and F7 1.5m Danish frames. In the diagram, stars with magnitudes brighter than $V = 16.5$ are those found in the frames taken at the Danish telescope, stars fainter than $V = 16.5$ are those in the NTT field.

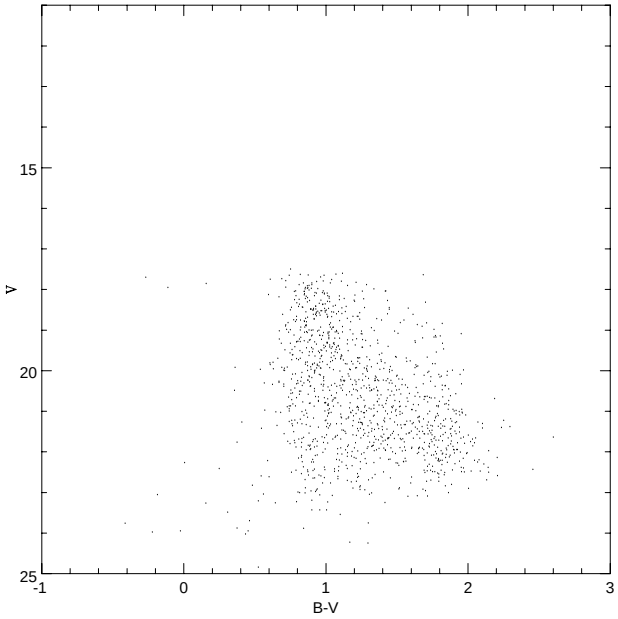

Fig. 2. Color–Magnitude diagram based on NTT observations for 1185 stars in a background field of NGC 3201.

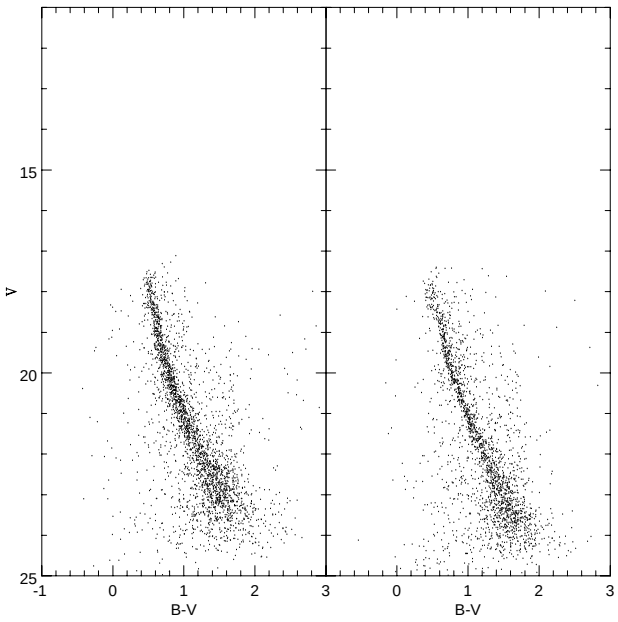

Fig. 3. Color–Magnitude diagram based on two 3.6m observations in NGC 3201 for 2890 stars (F3, left) and 2355 stars (F4, right).

in many stages in order not to modify the crowding level. The simulated c–m diagram, shown in Fig. 4, was obtained reducing the data in the same way as science data. In this last case we expect a larger error for the measured magnitudes than the statistical Poissonian error of the photon number. In fact, the crowding level can act to enlarge the final error causing a less accurate profile fitting. The width of the MS at V = 18 ÷ 18.5 is, in Fig. 1, $\sim 0.08 \div 0.09$ mag while the width of the simulated MS is slightly larger than ~ 0.03 mag. Considering only the statistical error reported by DAOPHOT II at this magnitude level B and V have similar errors of the order of ~ 0.015 mag. Therefore, we should expect a MS width of ~ 0.02 mag.

Analogous simulations were performed to obtain data shown in Figs. 5 and 6. They were analysed in order to estimate both the photometric error and the completeness correction, that is the percentage of stars found with respect the total number of added stars (see Sect. 4). The errors increase with the magnitude and are not Gaussian but strongly asymmetric. These effects, as expected, are due to the crowding that makes difficult to estimate the actual magnitude of a star when it is located in the wings of a brighter one. The B frames for the F2 field are also much less deep than the V frames. The latter are, instead, comparable for all the considered fields.

The larger width of the MS with respect to that obtained by the simulations can be due to many factors; a metallicity distribution of the stars in the cluster, a parallel binary sequence, an uncertainty in the determination of the image star centroid positions. This last factor affects the ability to identify stars in the two frames and can be considered dominant for the larger magnitudes. In fact, a large part of points observed far from the MS is due to different stars erroneously identified as the same star in the two color frames (Fig. 1). However, the presence of a parallel sequence of binaries can not be discarded since there is a large number of BSSs (Sect. 3.7). On the contrary, we did not find evidences for a metallicity spread among red giant stars.

3.1. Previously determined fiducial sequences

Among the most recent photometric observations in NGC 3201, we report here the results determined by Brewer et al. 1993 and

Table 3. Fiducial sequences for the c–m diagrams in Fig. 1.

BV_{MS-RGB}	V_{MS-RGB}	BV_{BS}	V_{BS}	BV_{HB}	V_{HB}
1.667	11.66			0.802	14.77
1.569	11.91			0.702	14.81
1.479	12.16			0.607	14.83
1.410	12.41			0.502	14.87
1.350	12.66				
1.290	12.91			0.401	14.75
1.250	13.16			0.301	14.76
1.200	13.41			0.201	14.76
1.160	13.66			0.101	14.81
1.135	13.91				
1.102	14.16				
1.078	14.41				
1.053	14.66				
1.025	14.91				
1.006	15.16				
0.984	15.41				
0.960	15.66	0.126	15.66		
0.944	15.91	0.171	15.91		
0.927	16.16	0.206	16.16		
0.916	16.41	0.266	16.41		
0.901	16.66	0.306	16.66		
0.891	16.91	0.351	16.91		
0.864	17.16	0.406	17.16		
0.823	17.41	0.452	17.41		
0.703	17.66				
0.667	17.91				
0.651	18.16				
0.654	18.41				
0.666	18.66				
0.681	18.91				
0.699	19.16				
0.722	19.41				
0.752	19.66				
0.800	19.91				
0.850	20.16				
0.891	20.41				
0.934	20.66				
0.996	20.91				
1.053	21.16				
1.118	21.41				
1.188	21.66				
1.248	21.91				

by Alcaino et al. 1989. The fiducial sequences computed in these papers compared with that computed by us are plotted in Fig. 7.

3.2. Reddening

Previous reddening estimates for NGC 3201 are reported in Table 1. Alcaino & Liller 1981 compared also the Giant–Branch (GB) of NGC 3201 with GB of clusters of similar metallicity obtaining $E_{(B-V)}$ = 0.19 ± 0.02. Lee 1977 derived a value of $E_{(B-V)}$ = 0.21 by two–color diagrams of field stars and the same value was adopted by Brewer et al. 1993. Zinn 1980 determined $E_{(B-V)}$ = 0.27 from integrated light in selected filter passbands. Since the intrinsic color of the RR Lyrae blue edge is $(B-V)_0$ = 0.17 (Sandage 1969) a measure of the color of the reddest Blue Horizontal–Branch (BHB) stars can allow one to compute the reddening. However, NGC 3201 does not have a well defined instability strip and we can only guess a red limit about $(B-V) \sim 0.40$ (Fig. 1). The corresponding reddening value would be $E_{(B-V)} \sim 0.23$. We eventually adopt Alcaino & Liller's value of $E_{(B-V)} = 0.22 \pm 0.03$ throughout the paper.

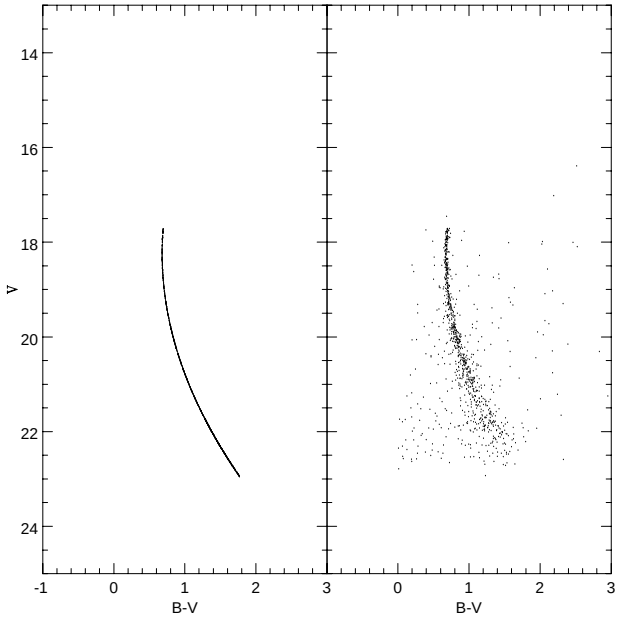

Fig. 4. Simulated Color–Magnitude diagram derived for the F2 NTT field. The input MS on the left was obtained by a simple parabolic interpolation. On the right the c–m diagram obtained with the same reduction of the science frames.

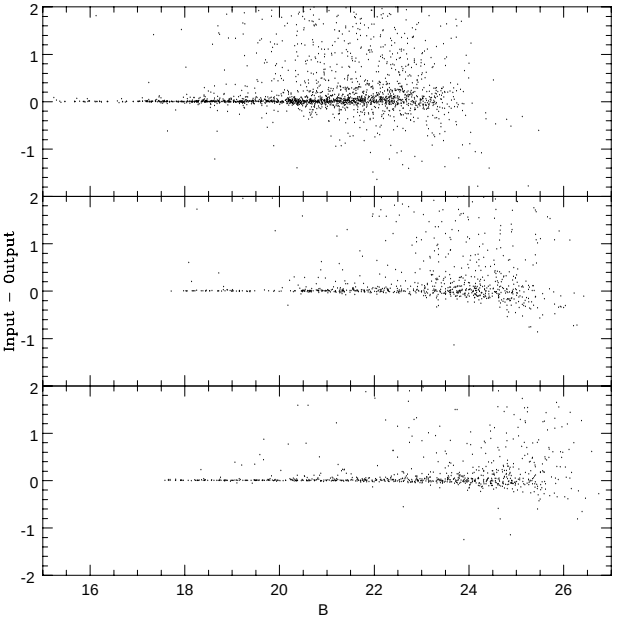

Fig. 5. B measured magnitudes for artificial stars versus difference with respect input magnitudes. Top: F2 NTT frame, middle: F3 3.6m frame, bottom: F4 3.6m frame.

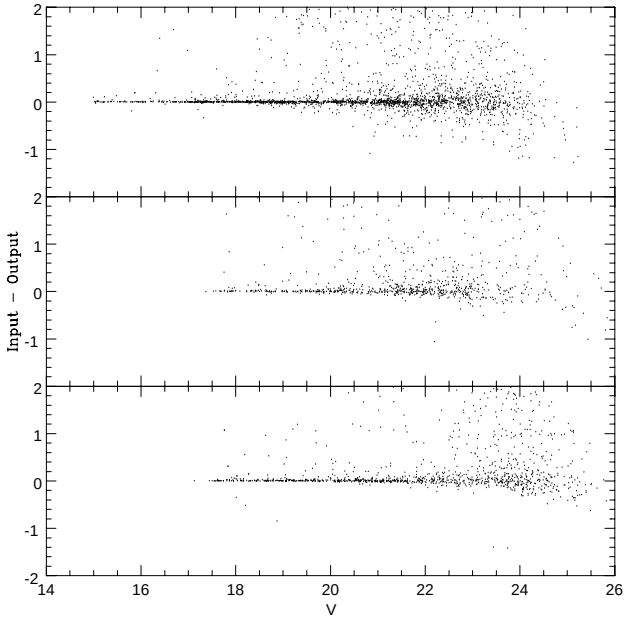

Fig. 6. V measured magnitudes for artificial stars versus difference with respect input magnitudes. Top: F2 NTT frame, middle: F3 3.6m frame, bottom: F4 3.6m frame.

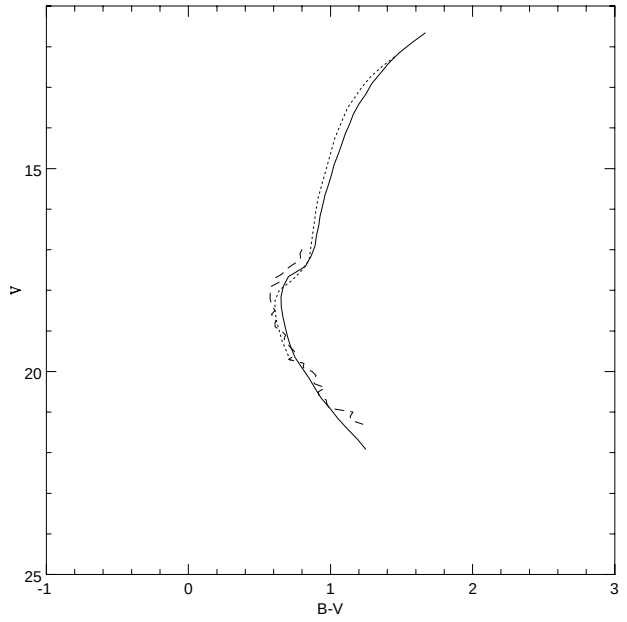

Fig. 7. Fiducial sequences determined by us (solid line), Brewer et al. 1993 (dashed), and Alcaino et al. 1989 (dot–dashed).

3.3. Metallicity

The metal content of NGC 3201 was determined by many authors and the estimates span a rather wide range. Harris & Canterna 1979 quoted $[Fe/H] = -1.26$, Zinn 1980, 1980b reported $[Fe/H] = -1.40$ and -1.51. Pilachowski et al. 1980 estimated $[Fe/H] \sim -1.0$. Pilachowski 1984 gave $[Fe/H] = -1.19$ while Zinn & West 1984 reported $[Fe/H] = -1.62$. From the Q_{39} index Zinn & West determined $[Fe/H] = -1.41$ and Gratton 1982, from high-dispersion spectroscopy, reported $[Fe/H] = -1.2$.

Table 4. Selected field subdwarfs from those reported in Stetson & Harris 1988 (a) and Laird et al. 1988 (b).

HD	M_V	$B-V$	$[Fe/H]$
a)			
25329	7.16	0.86	-1.33
103095	6.77	0.75	-1.36
134439	7.04	0.76	-1.40
134440	7.41	0.87	-1.52
201891	5.10	0.51	-1.42
b)			
25329	7.17 ± 0.20	0.865	-1.33
103095	6.76 ± 0.09	0.750	-1.36
134439	6.98 ± 0.18	0.760	-1.46
134440	7.36 ± 0.18	0.850	-1.34
201891	5.43 ± 0.32	0.510	-1.42

From the c–m diagram in Fig. 1 we estimated the RGB color at the HB level (Sect. 3.4) as $(B-V)_g = 1.01 \pm 0.03$. With the adopted reddening (Sect. 3.2) of 0.22 ± 0.03 mag this gets $(B-V)_{0,g} = 0.79 \pm 0.04$ in fairly good agreement with the values reported in Table 1. Finally, by the relation:

$$[Fe/H] = 2.85(\pm 0.37) \cdot (B-V)_{0,g} - 3.76(\pm 0.31), \qquad (3)$$

which has a rms error of 0.17 dex (Gratton 1989), we get $[Fe/H] = -1.51 \pm 0.20$ in agreement with the previous estimates. Another well known metallicity parameter is the magnitude difference between the HB and a point on the RGB at $(B-V)_0 = 1.4$. With the adopted reddening we obtain 2.95 ± 0.20 mag, still in good agreement with previous determinations (see Table 1). Applying the relation reported by Gratton 1989:

$$[Fe/H] = -0.65(\pm 0.08) \cdot \Delta V_{1.4} + 0.28(\pm 0.21), \qquad (4)$$

which has a rms error of 0.17 dex, we get $[Fe/H] = -1.64 \pm 0.20$, a value about the top range of metallicity for this clusters. Actually, as shown in Fig. 4e in Gratton 1989, $\Delta V_{1.4}$ tends to saturate toward the low metallicity regime.

Therefore, there is a wide range of metallicity estimates, running from $[Fe/H] \sim -1.0$ to $[Fe/H] \sim -1.6$, depending on the methodology and/or calibration applied. However, high–dispersion spectroscopy (Gratton 1982) seems rather to indicate a value closer to the lower limit of the range. As shown later on (Sect. 3.6), isochrone interpolation gives a value of $[Fe/H] \simeq -1.35$, in agreement, within the observational uncertainties, with most of the previous estimates.

3.4. Distance

The determination of GC distances is still affected by large uncertainties. There are a few methods for estimating the distance to GCs. We will determine distance moduli by MS fitting to the subdwarf sequence and by the $M_V - [Fe/H]$ relation for RR Lyrae stars.

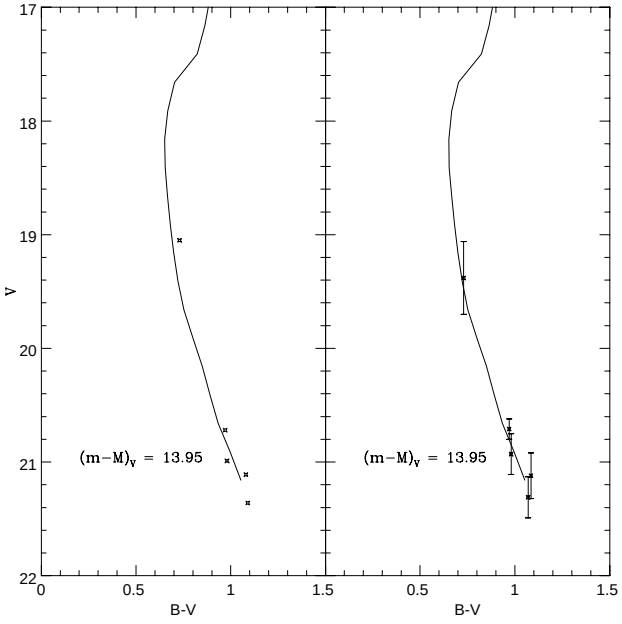

Fig. 8. Fit of the fiducial sequence of NGC 3201 to field subdwarfs of comparable metallicity. Left: data from Stetson & Harris 1988. Right: data from Laird et al. 1988.

3.4.1. Subdwarf fitting

One of the most widely used method to determine distance moduli of GCs is the MS fitting of the cluster to local halo subdwarfs with known (and comparable) metallicity and accurate parallaxes. A list of eight halo subdwarfs with $[Fe/H] \leq -1.3$ was provided by Carney 1979. However, since parameters for these stars were revised we use the values reported in Stetson & Harris 1988. In order to avoid metallicity corrections, among the stars reported we choose the five ones with metal content $[Fe/H]$ similar to that determined in Sect. 3.3. Data for these stars are reported in Table 4.

The color of each star was corrected for the adopted reddening (Table 5) leaving the distance modulus $(m-M)_V$ as a free parameter. The fiducial NGC 3201 sequence was then shifted until a satisfactory fit was obtained. The fit procedure gave us a distance modulus, not corrected for absorption, of $(m-M)_v = 13.95 \pm 0.15$. The same procedure was applied to data for just the same stars reported by Laird et al. 1988 still obtaining the same value of the distance modulus. The resulting fits are plotted in Figs. 8

Lutz et al. 1988 used 50 field subdwarf with accurate trigonometric parallaxes and spectroscopic $[Fe/H]$ to derive the formula:

$$M_V = 1.41 + 5.17 \cdot (B-V) - 0.94 \cdot [Fe/H] \quad (5)$$

relative to a Population II fiducial. The distance modulus of NGC 3201 was determined by translating the fiducial line until it coincides with the relation 5. The computed distance modulus, not corrected for absorption, is $(m-M)_V = 14.15 \pm 0.15$, in mild disagreement with the values determined with the other subdwarf fitting.

Table 5. Adopted and computed parameters in this work from c–m diagrams of NGC 3201.

parameter	value	note
$E_{(B-V)}$	0.22 ± 0.03	adopted
$(B-V)_g$	1.01 ± 0.03	
$(B-V)_{0,g}$	0.79 ± 0.04	
$\Delta V_{1.4}$	2.94 ± 0.20	
$[Fe/H]$	-1.51 ± 0.20	from $(B-V)_{0,g}$
$[Fe/H]$	-1.64 ± 0.20	from $\Delta V_{1.4}$
V_{HB}	14.75 ± 0.15	
$(m-M)_V$	13.95 ± 0.15	subdwarf fitting
$(m-M)_V$	14.15 ± 0.15	subdwarf fiducial fitting
$(m-M)_V$	14.0 ± 0.2	HB luminosity and calibration by Harris et al. 1991, Sandage & Cacciari 1990, and Carney et al. 1992
$(m-M)_V$	14.2 ± 0.2	HB luminosity and calibration by Sandage & Tammann 1995
$d_\odot$ (kpc)	4.6 ± 0.3	$(m-M)_V = 14.0$
$d_\odot$ (kpc)	5.0 ± 0.4	$(m-M)_V = 14.2$
V_{TO}	18.15 ± 0.15	
$(B-V)_{TO}$	0.65 ± 0.03	
$R(\frac{n_{HB}}{n_{RGB}})$	1.44 ± 0.21	
$R'(\frac{n_{HB}}{n_{RGB+AGB}})$	1.19 ± 0.16	
τ (Gyr)	14.5 ± 0.1	DM = 14.2
x	0.6 ± 0.3	$0.5 \leq M/M_\odot \leq 0.8$
x	1.7 ± 0.5	$M/M_\odot \leq 0.4 \div 0.5$
x_g	0.2 ± 0.4	$0.5 \leq M/M_\odot \leq 0.8$
x_g	1.0 ± 0.5	$M/M_\odot \leq 0.4 \div 0.5$

Table 6. Parameters, following some recent calibrations, for the relation between RR Lyrae luminosity and metal content.

α	β	reference
0.20	1.00	1) Harris et al. 1991
0.30	0.94	2) Sandage & Tammann 1995
0.25	1.09	3) Sandage & Cacciari 1990, Carney et al. 1992
0.18	095	4) Theoretical ZAHB

3.4.2. RR Lyrae calibration

A calibration of the absolute magnitude of RR Lyrae stars is a very common tool to compute GC distances. A widely used approach is to consider the mean luminosity constant, $M_V \simeq$ +0.6 and consequently to determine the distance modulus. We estimate $V_{HB} = 14.75 \pm 0.15$ (Fig. 1). This value is in a fairly good agreement with most previous determinations as shown in Table 1. Assuming a constant HB luminosity a distance modulus $(m-M)_V = 14.15 \pm 0.15$ is computed. Actually, as shown by most recent studies, the mean RR Lyrae luminosity varies with metallicity according to:

$$M_{V,RR} = \alpha \cdot [Fe/H] + \beta. \quad (6)$$

There are four primary methods to determine the parameters α and β of Eq. (6): statistical parallaxes, GC MS fitting, the Baade–Wesselink method, and theoretical models. As reviewed by Renzini & Fusi Pecci 1988 the question is far from

being solved (see also Durrel & Harris 1993). However, the computed HB luminosities at $[Fe/H] = -1.41$ range between $0.7 \div 0.9$ mag, with an error of at least 0.15 mag. Among the most recent calibrations we consider those reported in Table 6 where also a theoretical relation is reported (Sweigart et al. 1987).

Assuming case 1), we get $M_V = 0.72$ at $[Fe/H] = -1.41$. Therefore we can compute a distance modulus of $(m-M)_V = 14.0 \pm 0.2$, in a good agreement with that determined by subdwarf fitting and marginally consistent with that determined by subdwarf fiducial. Otherwise, if we adopt the relation 2) we obtain $M_V = 0.52$ and $(m-M)_V = 14.2 \pm 0.2$, in agreement with subdwarf fiducial fitting. Finally, by relation 3) we get $M_V = 0.74$ and $(m-M)_V = 14.0 \pm 0.2$ once again supporting a "short" distance modulus.

Summing up, we get essentially two values for the NGC 3201 distance modulus: $(m-M)_V = 14.0$ and 14.2. Assuming $A_V/E_{(B-V)} = 3.2$ we deduce $(m-M)_0 = 13.3 \pm 0.15$ and $(m-M)_0 = 13.50 \pm 0.2$, respectively. This corresponds to $d_\odot = 4.6 \pm 0.3$ Kpc and $d_\odot = 5.0 \pm 0.4$ Kpc.

Alcaino & Liller 1981 estimated the distance modulus by adopting an average brightness for the RR Lyrae variables of $V = 14.67$. They used $M_V = +0.6$ and obtained $(m-M)_V = 14.07 \pm 0.15$. Brewer et al. 1993, instead, obtained $(m-M)_V = 14.2 \pm 0.15$ fitting a subdwarf fiducial (Lutz et al. 1988) to their MS, in fairly good agreement with our estimate with the same methodology. Using the HB level in the relation between RR Lyrae absolute luminosity and metallicity derived by Jones et al. 1992 (based on Baade–Wesselink method), Brewer et al. 1993 determined a distance modulus of 14.0 ± 0.16. Thus, their results agree with ours. In the following, we consider both the determined distance modulus values.

3.5. Turnoff

From the color–magnitude in Fig. 1 we derive a TO location such as $V_{TO} = 18.15 \pm 0.15$ and $(B-V)_{TO} = 0.65 \pm 0.03$. As shown in Table 1 and in Fig. 7, Brewer et al. 1993 found a TO fainter and slightly bluer. The TO position reported by Alcaino et al. 1989 is almost at the same luminosity but 0.08 mag bluer in $(B-V)$.

3.6. Age

Alcaino & Liller 1981 deduced an age of 12.2 ± 2 Gyr from the Demarque & McClure 1977 isochrones with $[Fe/H] = -1.4$ and $Y = 0.3$. Alcaino et al. 1989 determined, instead, an age of 16.3 ± 3 Gyr by fitting VandenBerg & Bell 1985 isochrones with a metal content $[Fe/H] = -1.27$.

In order to determine the age of a cluster by isochrone fitting, we need to know the MS TO position, the distance, the helium content, and the metal abundance. The turnoff position was estimated in Sect. 3.5 while the distance modulus in Sect. 3.4. The metal content Z was discussed in Sect. 3.3 to be in the range $Z = 0.0005 \div 0.001$. The helium content is assumed to be $Y \simeq 0.235$, according to the Buzzoni et al. 1983 calibration and adequate for the reported metal content. In any case, following the same paper, we computed the ratio R and R' as well. The values obtained, $R = 1.44 \pm 0.21$ and $R' = 1.19 \pm 0.16$, are in almost perfect agreement with the data reported by Buzzoni et al. 1983.

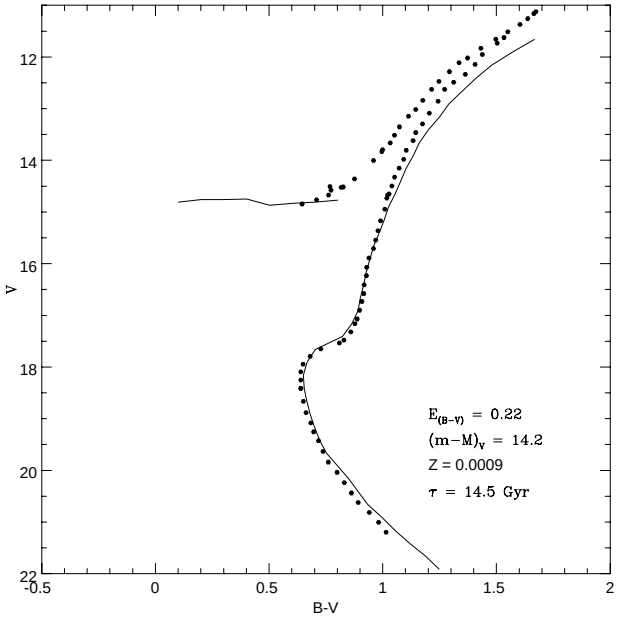

Fig. 9. Isochrone fitting on NGC 3201 fiducial line. Main–Sequence, Giant and Horizontal Branches are shown. The model is an interpolation between those computed by Fagotto et al. 1994a, 1994b for $Z = 0.0004, Y = 0.23$ and $Z = 0.004, Y = 0.24$.

To obtain meaningful results we should avoid the introduction of intrinsic biases following from the application of inhomogeneous or incomplete grids. We should consider models which provide a data–base of firstly complete in mass, chemical composition, and major evolutionary stages, and secondly homogeneous as well up to date in its physical ingredients, namely opacity, nuclear reaction rates, neutrino energy losses, mass–loss rates, equation of state, etc. The stellar models published by the "Padova group" meet the previous requirements. We considered the models computed by Fagotto et al. 1994a, 1994b for $Z = 0.0004, Y = 0.23$ and $Z = 0.004, Y = 0.24$ which are calculated with mild core and envelope overshooting and by the recent radiative opacities by the Livermore Group (Iglesias et al. 1992). For further details on the physical assumptions see Bressan et al. 1993.

By a linear interpolation on the grid for $Z = 0.0004$ and $Z = 0.004$ we found that the best fit of NGC 3201 fiducial sequence with models is obtained with a metal content $Z = 0.0009$ ($[Fe/H] = -1.35$). We succeeded to satisfactory fit the main sequence and the horizontal branch luminosity only with a distance modulus of 14.2. The age deduced is therefore $\tau = 14.5 \pm 1$ Gyr (Fig. 9). The error is only relative to the fit procedure and does not take into account the uncertainties relative to each parameter involved. The disagreement at the highest luminosity between model and data is probably due to saturation effects of the brightest stars in our sample.

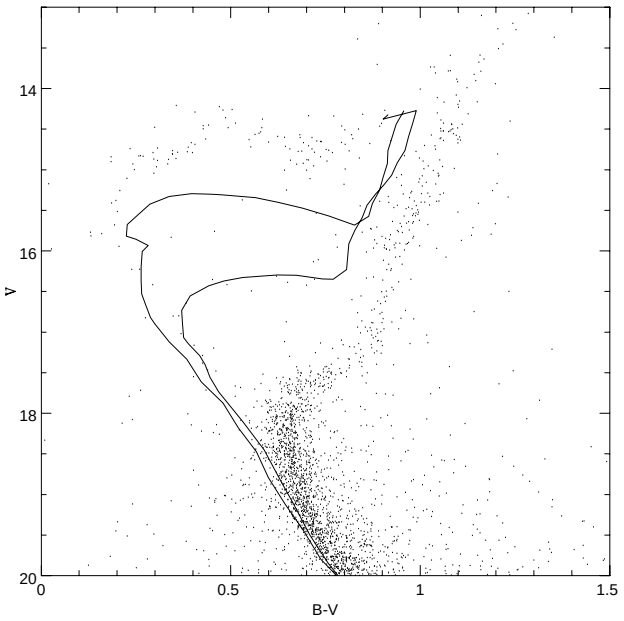

Fig. 10. The upper NGC 3201 c–m diagram. A region from $\sim$ 2 mag below the MS TO up to $\sim$ 1.5 mag above the HB is shown. Some blue stragglers defining a sequence going up almost to the blue HB tail is clearly visible. Continuum lines are two isochrones computed for 1.6 and 3.2 Gyr. Most of the BSs follow the 3.2 Gyr isochrones, but some better follow the 1.6 Gyr. Some probable progeny of the BSSs is also present.

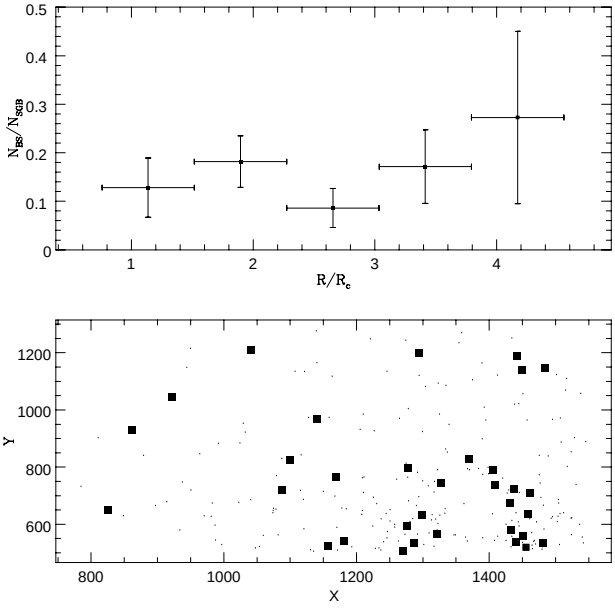

Fig. 11. Spatial concentration of BSSs found in the F2 field with respect SGB stars in the same field. NGC 3201 core radius, R_c, from Trager et al. 1993

No satisfactory fit was obtained with a distance modulus of 14.0 mag. Using Buonanno et al.'s 1993 fitting function of the VandenBerg & Bell 1985 isochrones for Y = 0.23 (their Eq. 1e) we derive an age of 12.3 Gyr.

3.7. Blue Stragglers

BSSs lie above the MS TO region in c–m diagrams, a region where normal stars should already have evolved away from the MS. There are three classical hypotheses on the nature of BSSs: that they represent single stars with extended MS lifetime, coalesced stars, or mass transfer in binaries. However, in globular cluster BSSs are commonly believed to be the result of physical coalescence in case of stellar collisions or of mass transfer in a primordial binary (Aurière et al. 1990, Stryker 1993 and reference therein). Therefore, BSSs can become tracers of binary populations in addition to providing an opportunity to learn how interactions in binary systems affect stellar evolution.

A sequence of BSSs is clearly discernible in Fig. 1. There are $\sim$ 40 stars bluer than the MS TO. Their sequence is quite narrow with respect to BSSs in other GCs, and seems to join the blue tail of the HB. A part of the whole c–m diagram of Fig. 1 is shown in Fig. 10. The plotted lines are isochrones for Z = 0.0009 with τ = 1.6 Gyr and τ = 3.2 Gyr. The isochrones superpose well to the BS sequence. The TO mass for NGC 3201, determined by an isochrone of τ = 14.5 Gyr (Sect. 3.6), is $\sim 0.8\,M_{\odot}$ while the TO masses for the τ = 1.6 and 3.2 Gyr are ~ 1.55 and $1.2\,M_{\odot}$. Therefore, the youngest isochrone has a TO mass almost twice the cluster TO mass. Both scenarios previously reminded can lead to such heavy stars. It is of course possible that some BSSs are field stars but the contamination at these magnitudes should be very small. Furthermore, the group of stars in the HB at $(B-V) \sim 0.75$ could be partly due to BSS progeny, that is stars that were formerly BSs. As pointed out by Fusi Pecci et al. 1992 there cold be a partial connection between the properties of BSSs and HB morphology.

Another important topic about BSSs is their relative concentration with respect to "normal" cluster stars. In Fig. 11 the spatial distribution of BSSs with respect to cluster stars at the same luminosity is shown. The concentration does not appear so strong as in NGC 6397 (Aurière et al. 1990) but there is a possible bimodal distribution as that put into evidence, even if much more defined, by Ferraro et al. 1993 in M3. Actually, it would need an analysis of a larger area of the cluster to put firm constraints on the spatial BSS distribution.

The existence of a BSS sequence was also found by Brewer et al. 1993 and suggested by Lee 1977.

4. Luminosity and mass function

The MF is one of the most fundamental parameters in the study of the evolution of star systems as open and globular clusters or even galaxies. The relative distribution of stellar masses is also a tool for estimating the total mass of stellar systems. In GCs, it allows one to study the physical characteristics of Low Mass Stars (LMS), roughly stars with masses lower than $\sim 0.6 M_{\odot}$.

Earlier works involving faint–star counts in GCs such as Fahlman et al. 1989 and Richer et al. 1991 have shown that the MFs of at least some GCs appear to be rising as the observations approach the brown–dwarf regime. Capaccioli et al.

1993 pointed out a relation between the MF slope and the height on the Galactic plane or the Galactocentric distance for a sample of GCs. Their MF slopes were measured in the range $0.5 \leq m/M_{\odot} \leq 0.8$. Stiavelli et al. 1991 suggested that this kind of relation can be the result of disc–shocking phenomena.

4.1. Luminosity function

The LFs determined from CCD detectors suffer from incompleteness which need to be corrected in order to derive the true LF. To evaluate the completeness of the star finding algorithm and the errors in the derived magnitudes, many artificial stars, with the same Point Spread Function (PSF) and known magnitude, were added to the science frames. These frames were processed in the same manner as the originals. In Figs. 4, 5 and 6 some results of these analyses are shown. By these techniques we got estimates of the errors associated to the measured magnitudes and a completeness function to correct the derived LF.

Among the various methodologies developed in the literature to perform the completeness correction two of the most rigorous are those described by Stetson & Harris 1988 and Drukier et al. 1988. However, both these techniques are difficult to apply. The first technique needs an "a priori" knowledge of the form of the actual LF while the second one needs a very large number of experiments as those which were carried out to produce Figs. 5 and 6. On the other hand, a very simple method, proposed by Mateo & Hodge 1987, consists in adding to the scientific frames artificial stars, reducing the frames in the same manner as the scientific ones, and determining the number of recovered stars for magnitude interval and, therefore, an estimate of the completeness correction function. This method has many advantages as it does not need neither an "a priori" knowledge of the form of the LF and a large number of numerical experiments. However, some improvements are possible especially when applied to star counts determined from c–m diagram, as this is the case. The reason to go on in this manner instead of determining the LF using star counts in just one color is that identifying stars in two almost independent images can reduce the errors associated to false detections of stars that at low luminosities become dominant.

In the recent literature there was a wide debate about completeness corrections. The fundamental point is to understand if completeness corrections obtained for LFs computed by frames taken in different colors are either independent (Mateo 1988) or dependent (Vallenari et al. 1992) on each other. In the first case the completeness correction in the c–m diagram is estimated by the product of those in the two colors involved; in the second, it is dominated by the strongest of them. In many papers the effects produced by the application of one or the other technique are evaluated (Sagar & Richtler 1991; Mateo 1992; Vallenari et al. 1994). In particular, in Vallenari et al. 1994, the effects of false detections due to the statistical fluctuation of the sky level and the full subject of completeness correction were also considered. The conclusions of that paper (see also Vallenari & Ortolani 1993) were that in a BV c–m diagram derived in strongly crowded fields the completeness factors are not independent. This conclusion is valid even for other colors if the spatial distribution of the luminous stars is essentially the same. This is due to the fact that the completeness correction is substantially dominated by the crowding rather than by the Poissonian noise on the image. Therefore, the lower completeness factor in either B or V is a good approximation of the actual crowding correction, while a correction based on the product of both the completeness function should strongly overestimate the result.

Table 7. LF in the F2 of NGC 3201. The counts are taken from the c–m diagram while the recovery factors are computed from the B exposures.

f	N	N_{corr}	$V(\pm 0.25)$
1.00 ± 0.316	6	6 ± 3	15.750
1.00 ± 0.208	23	23 ± 7	16.000
1.00 ± 0.145	35	35 ± 8	16.250
0.93 ± 0.122	35	38 ± 8	16.500
0.92 ± 0.130	43	47 ± 10	16.750
1.01 ± 0.137	54	53 ± 10	17.000
1.01 ± 0.137	68	67 ± 12	17.250
0.96 ± 0.101	145	151 ± 20	17.500
0.93 ± 0.093	223	240 ± 29	17.750
0.91 ± 0.100	290	319 ± 40	18.000
0.86 ± 0.094	360	419 ± 51	18.250
0.95 ± 0.100	391	412 ± 48	18.500
0.96 ± 0.103	439	457 ± 54	18.750
0.89 ± 0.095	505	567 ± 66	19.000
0.92 ± 0.087	586	637 ± 66	19.250
0.84 ± 0.067	591	704 ± 63	19.500
0.87 ± 0.064	607	698 ± 59	19.750
0.84 ± 0.063	661	787 ± 66	20.000
0.89 ± 0.064	669	752 ± 61	20.250
0.74 ± 0.052	708	957 ± 76	20.500
0.72 ± 0.053	676	939 ± 78	20.750
0.74 ± 0.057	592	800 ± 70	21.000
0.70 ± 0.053	533	761 ± 66	21.250
0.66 ± 0.052	488	739 ± 67	21.500
0.46 ± 0.045	472	1026 ± 111	21.750
0.46 ± 0.049	440	957 ± 112	22.000
0.36 ± 0.046	403	1119 ± 154	22.250
0.22 ± 0.042	336	1488 ± 303	22.500

In this paper we have followed the same procedure. The dominant completeness factor was always that associated with the B frames. The LF determined in fields F2, "background", F3 and F4 are reported in Tables 7, 8, 9, and 10. Counts are computed in binsize of 0.5 mag determined at steps of 0.25 mag.

The final LFs corrected for background contamination are given in Table 11. For the deepest fields we have extrapolated the "background" field LF by the tables of Ratnatunga & Bahcall 1985, after testing the consistency with observed number of field stars in the "background" field and on the red side of the MS (see also Ortolani & Rosino 1987; Ortolani 1988). In detail, since data for NGC 3201 are not contained in Ratnatunga & Bahcall's paper we considered the predicted star counts for NGC 2808, a GC with similar Galactic longitude and latitude ($l_{II} = 282.192, b_{II} = -11.253$ Djorgovski & Meylan 1993) to NGC 3201. Galaxy models are in fact implicitly symmetric

Table 8. LF in the NTT background field of NGC 3201. The counts are taken from the c–m diagram while the recovery factors are computed from the B exposures.

f	N	N_{corr}	$V(\pm 0.25)$
0.94 ± 0.223	11	12 ± 4	17.500
1.00 ± 0.213	38	38 ± 10	17.750
1.00 ± 0.208	58	58 ± 14	18.000
1.04 ± 0.204	70	67 ± 15	18.250
1.00 ± 0.166	82	82 ± 16	18.500
0.91 ± 0.138	80	88 ± 17	18.750
1.00 ± 0.141	88	88 ± 16	19.000
1.07 ± 0.168	101	94 ± 18	19.250
1.00 ± 0.169	97	97 ± 19	19.500
1.00 ± 0.130	113	113 ± 18	19.750
0.96 ± 0.126	125	130 ± 21	20.000
0.98 ± 0.128	130	133 ± 21	20.250
0.98 ± 0.114	128	131 ± 19	20.500
0.96 ± 0.105	131	136 ± 19	20.750
0.98 ± 0.114	144	147 ± 21	21.000
0.94 ± 0.102	154	164 ± 22	21.250
0.93 ± 0.112	163	175 ± 25	21.500
0.82 ± 0.109	157	191 ± 30	21.750
0.82 ± 0.119	139	170 ± 28	22.000
0.83 ± 0.130	111	134 ± 24	22.250
0.82 ± 0.155	87	106 ± 23	22.500
0.84 ± 0.210	59	70 ± 20	22.750
0.71 ± 0.225	39	55 ± 20	23.000
0.42 ± 0.247	24	57 ± 36	23.250

with respect to the Galaxy plane. We then calculated the expected background stars extrapolating data shown in Table 8. Since Ratnatunga & Bahcall's counts have a bin width of 2 mag this extrapolation cannot be extremely effective and LF data at the lowest luminosities should be considered with some care. In any case our extrapolation yields in the background field 712 objects within the magnitude bin 21–23, and 1269 objects within the magnitude bin 23–25. The expected background counts in both the F3 and F4 fields are therefore 103 and 184, respectively. This means that, for the faintest 0.5 mag wide bins reported in Table 11, the background correction should consist of less then $\sim$ 50 objects assuming a simple linear relation between magnitude and star counts. This value should be compared with the number of detected stars that is always larger than $\sim$ 1000. Therefore, since our fields are not very far from the cluster centre, even an error of a factor of 2–3 in background estimation does not substantially affect our later conclusions.

Fig. 12 shows the LFs determined in this paper and, for comparison, that one of Brewer et al. 1993. The global shapes are essentially the same. Besides, the availability of many independent LF with different faint magnitude levels allows one to verify that the applied completeness correction procedure was essentially correct. The shapes of the deepest LFs in regions where the completeness corrections are still small (see Tables 7–10) confirm the less deep LFs in regions where they are already strongly corrected.

Table 9. LF in the F3 field of NGC 3201. The counts are taken from the c–m diagram while the recovery factors are computed from the B exposures.

f	N	N_{corr}	$V(\pm 0.25)$
1.00 ± 0.35	29	29 ± 12	17.500
1.00 ± 0.27	65	65 ± 19	17.750
0.86 ± 0.25	89	103 ± 32	18.000
0.94 ± 0.24	110	117 ± 32	18.250
0.95 ± 0.23	144	151 ± 39	18.500
1.00 ± 0.38	152	152 ± 59	18.750
0.71 ± 0.32	153	214 ± 97	19.000
1.00 ± 0.33	196	196 ± 67	19.250
1.20 ± 0.28	215	178 ± 44	19.500
0.94 ± 0.16	215	228 ± 43	19.750
0.91 ± 0.14	237	258 ± 44	20.000
0.93 ± 0.15	242	259 ± 45	20.250
0.93 ± 0.14	258	276 ± 46	20.500
0.80 ± 0.13	261	324 ± 57	20.750
0.83 ± 0.13	259	305 ± 53	21.000
0.90 ± 0.15	296	322 ± 55	21.250
0.76 ± 0.13	292	375 ± 70	21.500
0.71 ± 0.13	288	397 ± 74	21.750
0.90 ± 0.12	319	356 ± 52	22.000
0.86 ± 0.10	359	421 ± 53	22.250
0.73 ± 0.08	380	530 ± 60	22.500
0.73 ± 0.08	385	540 ± 60	22.750
0.54 ± 0.06	425	742 ± 98	23.000
0.53 ± 0.07	454	815 ± 110	23.250
0.46 ± 0.07	464	958 ± 152	23.500
0.25 ± 0.07	516	2025 ± 602	23.750
0.28 ± 0.07	509	1761 ± 550	24.000
0.13 ± 0.06	418	3139 ± 1429	24.250

4.2. Mass Function

To convert a LF into a MF we need to use a Mass–Luminosity Relation (MLR). A MLR is sensitive to metallicity, which also affects the bolometric luminosity and the spectral distribution of a star. The adopted MLR is that of Drukier et al. 1988, obtained by the isochrones of VandenBerg & Bell 1985 for 16 Gyr and for a metallicity $[Fe/H] = -1.27$ and extended down to a mass of $0.15\,M_{\odot}$. We chose to use these isochrones in order to safely compare our results with those of Brewer et al. 1993. Actually, some different results could be obtained by applying the recent isochrones by D'Antona & Mazzitelli 1995. They computed MLRs for an age of 10 Gyr and for four metallicities. Comparing the MLR for $Z = 0.001$ there is an almost constant difference of $\sim$ 0.4 mag in M_V. The isochrone of D'Antona and Mazzitelli 1995 ascribes a larger luminosity to a star at a given mass. On the contrary, the slope and the main features of both sets of isochrones seems to be the same. Besides, even taking into account the age difference, the resulting D'Antona & Mazzitelli's isochrone should become brighter by ~ 0.1 mag. In any case, this should affect only the value of the lowest observed masses both in our and previous photometry. The slope and the global features of the derived MFs would not be substantially changed by the aforementioned discrepancy.

Table 10. LF in the F4 field of NGC 3201. The counts are taken from the c–m diagram while the recovery factors are computed from the B exposures.

f	N	N_{corr}	$V(\pm 0.25)$
0.80 ± 0.18	32	40 ± 11	17.750
0.89 ± 0.18	70	79 ± 18	18.000
0.92 ± 0.19	82	89 ± 21	18.250
0.96 ± 0.20	81	84 ± 20	18.500
0.89 ± 0.18	97	109 ± 24	18.750
0.86 ± 0.17	111	129 ± 28	19.000
0.92 ± 0.19	122	133 ± 29	19.250
0.83 ± 0.16	128	154 ± 33	19.500
0.90 ± 0.15	143	159 ± 30	19.750
0.94 ± 0.16	164	174 ± 33	20.000
0.92 ± 0.15	163	177 ± 32	20.250
0.92 ± 0.16	149	162 ± 30	20.500
0.82 ± 0.14	136	166 ± 32	20.750
0.85 ± 0.14	157	179 ± 34	21.000
0.88 ± 0.14	191	213 ± 39	21.250
0.93 ± 0.14	191	200 ± 35	21.500
0.94 ± 0.13	185	194 ± 30	21.750
0.96 ± 0.13	199	209 ± 32	22.000
0.80 ± 0.11	214	273 ± 41	22.250
0.64 ± 0.08	253	408 ± 56	22.500
0.76 ± 0.09	287	394 ± 51	22.750
0.79 ± 0.09	290	335 ± 48	23.000
0.68 ± 0.08	344	472 ± 64	23.250
0.53 ± 0.07	405	727 ± 109	23.500
0.54 ± 0.08	416	731 ± 120	23.750
0.30 ± 0.06	448	1452 ± 312	24.000
0.15 ± 0.04	459	3022 ± 849	24.250

Table 11. Final V LFs corrected for background contamination.

V	$N(F2)$	$N(F3)$	$N(F4)$
17.50	147 ± 20	16 ± 13	
17.75	228 ± 19	52 ± 19	27 ± 13
18.00	301 ± 40	88 ± 32	64 ± 19
18.25	398 ± 51	102 ± 32	74 ± 22
18.50	386 ± 48	138 ± 39	71 ± 21
18.75	429 ± 54	139 ± 59	96 ± 25
19.00	539 ± 66	199 ± 97	114 ± 29
19.25	607 ± 66	181 ± 67	118 ± 30
19.50	673 ± 63	160 ± 44	136 ± 34
19.75	662 ± 59	208 ± 43	139 ± 31
20.00	746 ± 46	239 ± 44	155 ± 34
20.25	710 ± 61	240 ± 45	158 ± 33
20.50	915 ± 76	255 ± 46	141 ± 31
20.75	896 ± 78	303 ± 57	145 ± 33
21.00	753 ± 70	289 ± 53	163 ± 35
21.25	709 ± 66	304 ± 55	195 ± 40
21.50	681 ± 67	354 ± 70	179 ± 36
21.75	965 ± 111	374 ± 74	171 ± 31
22.00	903 ± 112	330 ± 52	183 ± 33
22.25	1076 ± 154	392 ± 53	244 ± 41
22.50	1421 ± 303	499 ± 60	377 ± 56
22.75		506 ± 60	360 ± 51
23.00		706 ± 98	299 ± 48
23.25		776 ± 110	433 ± 64
23.50		917 ± 152	686 ± 109
23.75		1981 ± 602	687 ± 120
24.00		1715 ± 550	1406 ± 312
24.25		3090 ± 1459	2973 ± 849

Our MFs are reported in Fig. 13 for each considered field, and are compared with the MFs derived by Brewer et al. 1993 in the V and I colors. We defined the differential mass function as dN/dM where N is the number of stars in each bin and M is mass. We count the stars in magnitude bins, using overlapping bins with a width of 0.5 mag and interval of 0.25 mag. The mass interval of a bin is calculated via the appropriate MLR, and divided into the number of stars in the bin.

The MFs show some common features. In the mass range $0.5 \leq M/M_{\odot} \leq 0.8$ they appear rather flat. Assuming that the MF can be fitted by a power law as $dN/dM \propto M^{-(1+x)}$ the index x assumes a value $x \simeq 0.6 \pm 0.3$.

Brewer et al. 1993 also quoted that there is a steep rise in the MFs below $\sim 0.4\,M_{\odot}$. We also found a similar behaviour. Discharging the last two bins in our F3 and F4 MFs, we get a slope $x \simeq 1.7 \pm 0.5$ for masses below $\sim 0.5\,M_{\odot}$, in fairly good agreement with the slope $x \simeq 1.5 \pm 0.4$ reported by Brewer et al. 1993. The rise of the MFs toward the smallest masses can be even steeper but we cannot say how safe can be our MFs at these masses because of possible not satisfactory background subtraction (see Sect. 4.1).

Such a steepening at $\sim 0.4\,M_{\odot}$ of the MF in globular clusters was not clearly detected by Paresce et al. 1995 and De Marchi & Paresce 1995a, 1995b. They quoted instead that MFs determined for NGC 6397, M 15 and 47 Tuc show a power–law increase in numbers for decreasing masses in the range $0.3 \leq M/M_{\odot} \leq 0.8$ but with a flattening below $\sim 0.25\,M_{\odot}$. Our data do not allow us to investigate the behaviour of globular cluster MFs in such a small mass regime.

The values of the MF slope also depend on the amount of mass segregation in NGC 3201. To compare results for NGC 3201 with other clusters one needs to determine a global value of the MF slope. With this purpose we have applied multimass King–Michie models with MFs approximated by power laws (Pryor et al. 1986). Depending on the central concentration Pryor et al. 1986 computed the global slope versus the apparent slope and the distance from the cluster centre in core radius units. Since the core radius for NGC 3201 is ~ 1.5 arcmin (Trager et al. 1993) our deepest frames have been observed at an average value of ~ 7 core radii from the cluster centre. Inspecting Pryor et al. 1986's Fig. 1 we obtain a global value of the MF slope $x_g \simeq 0.2 \pm 0.4$ in the mass range $0.5 \leq M/M_{\odot} \leq 0.8$ and a global slope $x_g = 1.0 \pm 0.5$ for the smallest masses.

Recently, Côté et al. 1995 found a MF slope of $x_g = 0.75 \pm 0.25$ studying the dynamics of NGC 3201, thus confirming the results derived by LF analyses.

These values are compatible with those derived from the relation computed by Capaccioli et al. 1993. For a cluster at Galactocentric distance around ~ 9 kpc and at a distance to the Galactic plane of ~ 1.3 kpc, the MF slope for masses in the range $0.5 \leq M/M_{\odot} \leq 0.8$ should be somewhat larger than

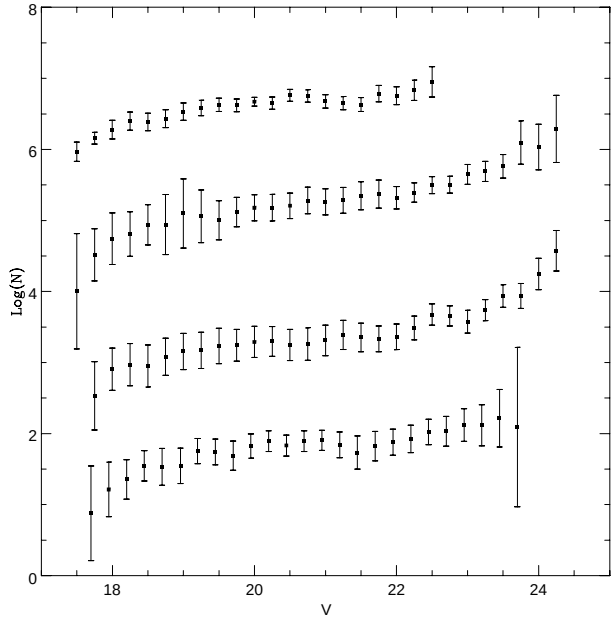

Fig. 12. Luminosity Functions derived by color–magnitude star counts in NGC 3201. Starting from the top: F2 field, F3 field, F4 field and, for comparison, LF derived by Brewer et al. 1993.

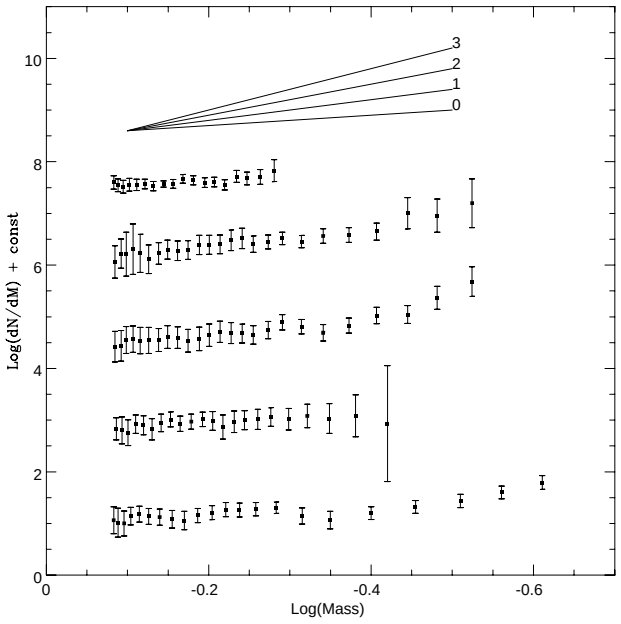

Fig. 13. Mass Functions derived by color–magnitude star counts in NGC 3201. Starting from the top: F2 field, F3 field, F4 field and, for comparison, V and I MFs derived by Brewer et al. 1993. Solid lines indicate mass functions with different values of the slope x.

zero. Things may be different for the global slopes for masses lower than 0.4 $M_\odot$ where this parameter should be rather larger. However, the relation shown by Capaccioli et al. 1993 (their Fig. 2) for the lowest masses has a large scatter and is not well defined. In any case, these results essentially confirm that MFs are related to the position in the Galactic gravitational field.

5. Conclusions

NGC 3201 is one of the most interesting Galactic globular cluster to observe. It is rather close to the Sun and with a fairly low concentration. These features allow us to study luminosity and mass function down to faint magnitudes.

We have determined c–m diagrams for various fields in the clusters and estimated reddening, metallicity, distance and age. The adopted value for the reddening is $E_{(B-V)} = 0.22 \pm 0.03$, while the metallicity is in the range $-1.3 < [Fe/H] < -1.6$. The distance modulus which allows one to correctly interpolate the MS, the RGB and the HB is $(m - M) = 14.2 \pm 0.2$. With this value the age is 14.5 ± 1 Gyr. A rather large number of BSSs are found in a very sharp sequence bluer than the cluster MS.

The study of the LFs obtained in different fields has confirmed the substantial validity of the methodology involved in completeness correction. The computed MFs are in substantial agreement among one other and with those previously determined in the literature for the same cluster even when computed with different procedures and instruments. The global slope of the MF, taking into account the mass segregation, is 0.2 ± 0.4 in the mass range $0.5 \leq M/M_\odot \leq 0.8$ and steeper toward decreasing masses.

A summary of the various parameters determined in this paper is reported in Table 5.

Acknowledgements. We thank the referee, T. Richtler, for his helpful comments and suggestions that we have included in the final version of our paper. SC thanks also the Osservatorio Astronomico di Brera–Milano for the kind hospitality.

References

Alcaino, G. 1976, A&AS, 26, 251
Alcaino, G., Liller, W. 1981, AJ, 86, 1480
Alcaino, G., Liller, W., Alvarado, F. 1989, A&A, 216, 68
Aurière, M., Ortolani, S., Lauzeral, C. 1990, Nature, 344, 638
Bressan, A., Fagotto, F., Bertelli, G., Chiosi, C. 1993, A&AS, 100, 647
Brewer, J.P., Fahlman, G.G., Richer, H.B., Searle, L., Thompson, I. 1993, AJ, 105, 2158
Buonanno, R., Corsi, C.E., Fusi Pecci, F., Richer, H.B., Fahlman, G.G. 1993, AJ, 105, 184
Buzzoni, A., Fusi Pecci, F., Buonanno, R., Corsi, C.E. 1983, A&A, 128, 94
Cacciari, C. 1984a, AJ, 89, 231
Cacciari, C. 1984b, AJ, 89, 1082
Capaccioli, M., Piotto, G., Stiavelli, M. 1993, MNRAS, 261, 819
Carney, B.W. 1979, ApJ, 233, 877
Carney, B.W., Storm, J., Jones, R.V. 1992, ApJ, 386, 663
Côté, P., Welch, D.L., Fischer, P., Gebhardt, K. 1995, ApJ, 454, 788
D'Antona, F., Mazzitelli, I. 1995, *private communication*
De Marchi G., Paresce F. 1995a, A&A, 304, 202
De Marchi G., Paresce F. 1995b, A&A, 304, 211
Demarque, P., McClure, R. 1977, in The Evolution of Galaxies and Stellar Populations, ed(s). B. Tinsley and R.B. Larson (Yale University Observatory, New Haven), 199
Djorgovski, S., Meylan, G. 1993, in Structure and Dynamics of Globular Clusters, ASP Conf. Series 50, ed(s). S.G. Djorgovski and G. Meylan, 325

Drukier, G.A., Fahlman, G.G., Richer, H.B. 1989, ApJ, 342, L27
Drukier, G.A., Fahlman, G.G., Richer, H.B., VandenBerg, D.A. 1988, AJ, 95, 1415
Durrel, P.R., Harris, W.E. 1993, AJ, 105, 1420
Fagotto, F., Bressan, A., Bertelli, G., Chiosi, C. 1994a, A&AS, 104, 365
Fagotto, F., Bressan, A., Bertelli, G., Chiosi, C. 1994b, A&AS, 105, 29
Fahlman, G.G., Richer, H.B., Searle, L., Thompson, I.B. 1989, ApJ, 343, L49
Ferraro, F.R., Fusi Pecci, F., Cacciari, C., Corsi, C., Buonanno, R., Fahlman, G.G., Richer, H.B. 1993, AJ, 106, 2324
Fusi Pecci, F., Ferraro, F., Corsi, C., Cacciari, C., Buonanno, R., 1992, AJ, 104, 1831
Gratton, R.G. 1982, A&A, 115, 171
Gratton, R.G. 1989, A&A, 211, 41
Harris, W.E., Allwright, J.W.B., Pritchet, C.J., van den Bergh, S., 1991, ApJS, 76, 115
Harris, W.E., Canterna, R. 1979, ApJ, 231, L19
Iglesias, C.A., Rogers, F.J., Wilson, B.G. 1992, ApJ, 397, 717
Jones, R.V., Carney, B.W., Storm, J., Latham, D.W. 1992, ApJ, 386, 646
Laird, J.B., Carney, B.W., Latham, D.W. 1992, AJ, 95, 1843
Landolt, A.V. 1983, AJ 88, 439
Lee, S.–W. 1977, A&AS, 28, 409
Lutz, T.E., Hanson, R.B., Van Altena, W.F. 1988, in The Extragalactic Distance Scale, ASP Conf. Ser. 4, ed(s). S. van den Bergh and C.J. Pritchett, 170
Mateo, M. 1988, AJ, 331, 261
Mateo, M. 1992, in The Globular Cluster Galaxy Connection, ASP Conf. Ser. 48, ed(s). G.H. Smith and J.P. Brodie, 387
Mateo, M., Hodge, P. 1987, ApJ, 320, 626
Menzies, J. 1967, Ph.D. thesis, Australian National University
Ortolani, S. 1988, in Harlow–Shapley Symposium on Globular Cluster Systems in Galaxies, IAU Symp. 126, 629
Ortolani, S., Rosino, L. 1987, A&A, 185, 102
Paresce F., De Marchi G., Romaniello M. 1995, ApJ, 440, 216
Penny, A.J. 1984, in Observational Tests of the Stellar Evolution Theory, IAU Symp. 105, ed(s). A. Maeder and A. Renzini (Dordrecht: Reidel), 157
Pilachowski, C.A. 1984, ApJ, 281, 614
Pilachowski, C.A., Sneden, C., Canterna, R. 1980, in Star Clusters, IAU Symp. 85, ed. J.E. Hesser, (Reidel:Dordrecht), 467
Pryor, C., Meylan, G. 1993, in Structure and Dynamics of Globular Clusters, ASP Conf. Series 50, ed(s). S.G. Djorgovski and G. Meylan, 357
Pryor, C., Smith, G.H., McClure, R.D. 1986, AJ, 92, 1358
Ratnatunga, K.U., Bahcall, J.N. 1985, ApJS, 59, 63
Renzini, A., Fusi Pecci, F. 1988, ARAA, 26, 199
Richer, H.B., Fahlman, G.G., Buonanno, R., Fusi Pecci, F., Searle, L., Thompson, I.B. 1991, ApJ, 381, 147
Sagar, R., Richtler, T. 1991, A&A, 250, 324
Sandage, A. 1969, ApJ, 157, 515
Sandage, A., Cacciari, C. 1990, ApJ, 350, 645
Sandage, A., Tammann, G.A. 1995, ApJ, 446, 1
Stetson, P.B. 1987, PASP, 99, 191
Stetson, P.B., Harris, W.E. 1988, AJ, 96, 909
Stiavelli, M., Piotto, G., Capaccioli, M., Ortolani, S. 1991, in Formation and Evolution of Star Clusters, ASP Conf. Ser. 13, ed. K. Janes, 449
Stryker, L.L. 1993, PASP, 692, 1081
Sweigart, A.V., Renzini, A., Tornambè, A. 1987, ApJ, 312, 762
Trager, S.C., Djorgovski, S., King, I.R. 1993, in Structure and Dynamics of Globular Clusters, ASP Conf. Series 50, ed(s). S.G. Djorgovski and G. Meylan, 347
Vallenari, A., Chiosi, C., Bertelli, G., Meylan, G., Ortolani, S. 1992, AJ, 104, 1100
Vallenari, A., Ortolani, S. 1993, in Data Analysis Workshop, 5^{th} ESO/ST–ECF, ed. P.J. Crosbol, 125
Vallenari, A., Ortolani, S., Chiosi, C. 1994, A&AS, 108, 571
VandenBerg, D.A., Bell, R.A. 1985, ApJSS, 58, 561
Webbink, R.F. 1985, in Dynamics of Star Clusters, IAU Symp. 113, ed(s). J. Goodman and P. Hut (Reidel: Dordrecht), 541
Zinn, R. 1980, ApJSS, 42, 19
Zinn, R. 1980b, ApJ, 241, 602
Zinn, R., West, M.J. 1984, ApJSS, 55, 45

This article was processed by the author using Springer-Verlag LaTeX A&A style file *L-AA* version 3.